EAI Endorsed Transactions
on Energy Web
Research Article EAI.EU

Embedded Highway Health Maintenance System Based on Digital Twin Superposition Model

Bijun Lei[1], Rui Li[2*] and Rong Huang[2]

[1]Wenshan Highway Bureau, Wenshan, China
[2]Kunming University of Science and Technology, Kunming, China

Abstract

INTRODUCTION: The highway monitoring data acquisition technology develops quickly. Based on the traditional form of continuous monitoring, intelligent management system focuses on digital and wireless transmission. In the operation of highway maintenance system, each system is independent of each other, lacking of effective connection. Moreover, the level of continuous monitoring is obviously backward, which restricts the development of highway health monitoring. It is necessary to further study the level of integration to achieve the real-time tracking and the monitoring of highway's healthy development.
OBJECTIVES: This paper presents a highway health maintenance system based on digital twin technology, which intends to provide a solution for efficient, stable and automatic data transmission of the highway operation and maintenance management.
METHODS: The output of the algorithm after the noise reduction effect is compared with the data containing the generated noise. The average number of nodes is set before running the algorithm to determine the actual length of the vertical position of the embedded sensor (calculating the position of two sensor nodes). The vertical length can be referred to the combined noise level formed and the combined test to determine the position. With the help of the overall data, it can be seen that the Kalman low-pass filtering algorithm can well describe the trend of the received signal and retain the key information in the received signal.
RESULTS: It proves that the algorithm in this paper has fast calculation speed and high efficiency, and the basic working principle is simple. Thus, it is a good data denoising solution.
CONCLUSION: The output in the paper ensures the data exchange and the update of the whole life cycle of highway, defines the digital twin entity model, and provides a reference for the establishment of information and data network.

Keywords: Highway monitoring, Embedded system, Data transmission, Digital twin model, Kalman filter

Received on 29 December 2023, accepted on 29 March 2024, published on 05 April 2024

doi: 10.4108/ew.5654

1. Introduction

With the innovative development concept of "digital highway" put forward by highway maintenance enterprises, the construction of highway digital platform by digital twin technology has become the most effective way. Digital twin technology highway architecture design is based on the digital twin of embedded monitoring equipment, which requires the physical monitoring system mapped by virtual digital space to realize the communication of the IOT monitoring system. However, the physical simulation model of the monitoring system through FEA (Finite Element Analysis) can not meet the needs of the digital twin technology of the automatic monitoring system. The performance in the fields of recognition, classification and NLP (Natural Language Processing) of display images has brought new opportunities to the physical model of automatic monitoring [2]. The DL (Deep Learning) data through intensive training has high security and can meet the requirements of the near real-time simulation model of the physical field in the monitoring system. It is of great significance to introduce DL into the embedded highway

*Corresponding author. Email: liruiking@kust.edu.cn

health maintenance system and use DL to carry out the physical simulation of the monitoring system [3].

The collection and selection of data related to digital twin technology from physical space to digital virtual network is the core of the practicality of industrial Internet technology. Digital and intelligent virtual models provide physical structural dimensions, and on this basis, other technologies are needed to compare the pair-mapping of information and data gradually formed in the process of data collection. G. Yu et al. use UWB technology to compare data acquisition and preliminary processing, to carry out real-time automatic location sensing and resource monitoring, and to promote highway safety management and pavement maintenance [4]. With the help of wireless acquisition technology, the field information such as static sensor search, data delay and data flow is analyzed. The highway structure information is reconstructed with the help of monitoring sensors. A. Brawn et al. collect field information through sensors laid on expressways, and then compares the data of multiple detection sensors by computer analysis technology to identify abnormal data and realize field safety management [5]. Based on a large number of relevant information collected by environmental detection sensors, the strategy of highway continuous monitoring is studied from the aspects of stability, reliability and relevance. Furthermore, a network model is constructed to achieve a real-time interconnected highway continuous monitoring program. Y. Lo. et al. create and establishes a highway health detection and alarm system through wireless network technology. They also compare various monitoring equipment placement strategies, and automatically obtain real-time location and time-related information from the system [6]. Although the above research has accumulated some basic knowledge of practice and theory, it has always lacked the establishment of a scientific and systematic common system of digital twin technology. Especially for solving the problem of efficient and stable data transmission environment, we need to combine the embedded system, wireless transmission control and driver management program to explore and study the effective management program step by step.

The highway maintenance system can not meet the requirements of the digital twin real-time simulation model of the equipment under the digital highway. This paper innovatively introduces the physical simulation space of the deep neural network monitoring system, and discusses the data security and standardization of the physical simulation deep neural network in the monitoring system. The Kalman filter algorithm is used to estimate the system state and its uncertainty step by step in the prediction operation, and the average reasoning is selected to give the prediction weight when the uncertainty increases. The algorithm recursion can automatically run the program in real time, selecting only the current input measurement value and the previously calculated normal state as well as the large uncertainty vector space.When additional historical data are needed, the physical characteristics of the algorithm make the memory occupation of the running program very small, which can support higher iteration frequency.

2. Highway health trend model

The embedded highway health maintenance system is closely related to the material and thickness requirements of highway pavement, ambient temperature, basic structure combination and surrounding traffic volume. The reason is that the factors for the gradual formation of different types of injuries are not exactly the same, which makes their normal state and future development trend different [7]. The development of the engagement state can be more accurately predicted by selecting different injury prediction maps for different types of injury engagement causes.

(1) Instability type damage (ΔB_R) is a very common type of damage and is more likely to occur under high temperature conditions. Considering that concrete mixture is a material requiring ambient temperature sensitivity, its road quality and performance are closely related to its ambient temperature sensitivity [8]. The ambient temperature will change with the passage of time. Under relatively stable high temperature conditions, the viscosity of concrete mixture decreases. The elastic modulus of stiffness decreases. The shear strength decreases, and the potential to withstand deformation also decreases [9]. Under the action of repeated vibration in the process of highway driving, transverse shear slow flow is easy to occur and gradually cause damage. It is because of the quality and performance of the concrete mixture itself and the high temperature conditions. The surrounding traffic conditions are not the important factors causing instability damage, including the surrounding traffic volume, the number of vehicle axles, the speed, the direct contact resistance of tires, etc. [10]. The calculation formula is as follows:

$$\Delta B_R = \sqrt{T_n \times T_d + W_d \times A_s} \tag{1}$$

In the formula, the added value is closely related to the general time interval T_n of axle load action, the external environment that impedes the ambient temperature T_d , and the required high temperature stability W_d and safety-related parameters A_s of the material.

(2) Foundation structure damage is (ΔB_U). The structural layer of asphalt pavement is not strong enough to withstand the vibration of motor vehicles. The bending deformation of foundation works and cement concrete pavement is transmitted vertically upward to the concrete base, and the overall structure of the road is caused by the bending deformation [11]. The deformation of flexible cement concrete pavement is large, and the foundation bearing capacity of soft soil cement concrete pavement and high fill cement concrete pavement are the factors causing damage to the foundation structure [12]. In addition, the relatively large axle load and the factors related to the vibration of the axle load and motor vehicles, such as the normal time interval, may cause such damage to the road during operation. However, the bearing capacity of the asphalt pavement structure, semi-rigid foundation engineering and road trenches, traffic light intersections and other foundations are relatively small, which are not easy to cause structural damage. However, the normal state of such

damage is closely related to the vibration of various road structures and motor vehicles [13]. The foundation bearing capacity of cement concrete pavement and base course is expressed by deflection, and the calculation formula is as follows:

$$\Delta B_U = -\sqrt{V_x \times H} \quad (2)$$

In the formula, the damage depth of foundation structure can be expressed by cumulative axle load interval V_x and deflection H.

(3) Compaction type damage (ΔB_z) is caused by insufficient concrete mix proportion, excessive temperature or improper design and construction of the required material quality and material quantity control structure layer during design and construction [14]. Improper design and construction pose a potential danger of sudden failure. However, in the initial stage of operation of the asphalt pavement network, the seismic effect of motor vehicles over time is moderate. The concrete mixture gradually disappears and is compacted. The gap outside it gradually disappears and shrinks, gradually forming a depression where the two wheels generally act [15]. The calculation formula is as follows:

$$\Delta B_z = \sqrt{J_m \times G_t} \quad (3)$$

Where, the specific surface area J_m of the concrete mixture and the speed G_t at which the damage depth increases can be accumulated on the shaft.

3. Model superposition of digital twin maintenance system

The highway embedded health maintenance system has many components, and the highway system components of the digital twin technology layer also contain many system components, which are composed of various main components. Since the loading and rendering of the Three. js is done in Java Script in the open model, it is important to refresh the model each time a system component is loaded [16]. This results in a complex environment structure for loading software programs for the entire highway system components.

To reduce the complexity of the original road maintenance system, the refresh frequency of the embedded system should be reduced, and multiple system components should be loaded. We adopt Ajax to load multiple system components asynchronously. In the process of Ajax loading, the component uses Ajax to connect the server cluster, and finally realizes the loading model and loads the data to the specified location. This technique can selectively update parts of the model that cannot be opened without reloading the entire model. Additionally, that asynchronous form of the operation occur during the execution of the program. When it executes synchronously, it waits for the task to be completed, and then continues to execute another final task until the task is completed. When an asynchronous operation is performed, it is able to continue another task before completing the task. In the context of an embedded system, synchronous and asynchronous operations can translate to the direct execution of a process or the completion of the last task on top of "multiple threads." A functional schematic of the system is shown in Figure 1.

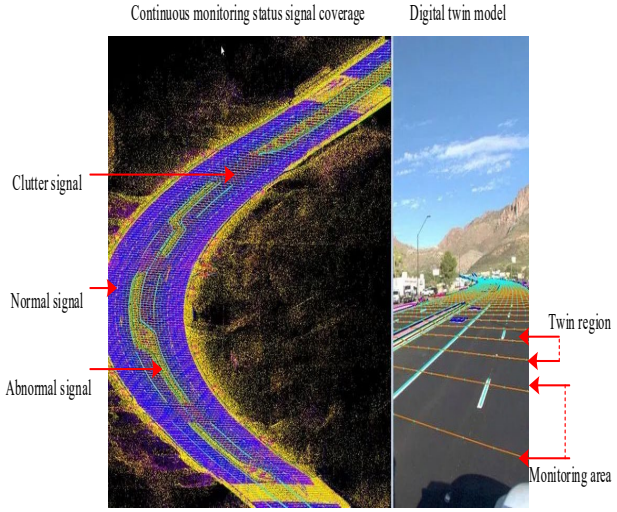

Figure 1. Function diagram of highway health monitoring system

Embedded systems simulate system synchronization and asynchrony by assigning time slices to different numbers of threads. A thread is a sequence of commands (a block of code) used to act as a unit of work. An embedded system is able to manage multiple threads to work in pairs before switching to another thread [17]. Allocate more threads to multiple threads to reduce processing time. In embedded systems, multitasking only needs to execute the above commands to complete and execute the next task to achieve high-speed data processing [18]. Figure 2 is a comparison of different communication mode.

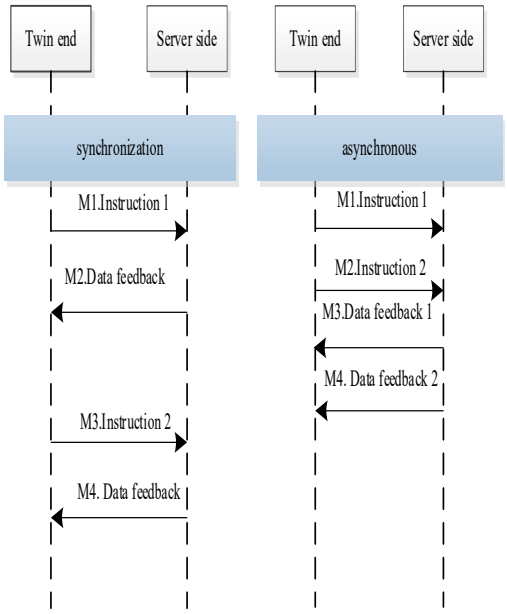

Figure 2. Transmission comparison of different communication modes

In Figure 2, the highway maintenance system components can be loaded synchronously and the highway maintenance system components can be loaded asynchronously.

Figure 3 shows the analysis times for the different models. Asynchronous operation loading mode is more competitive than synchronous loading time [19].

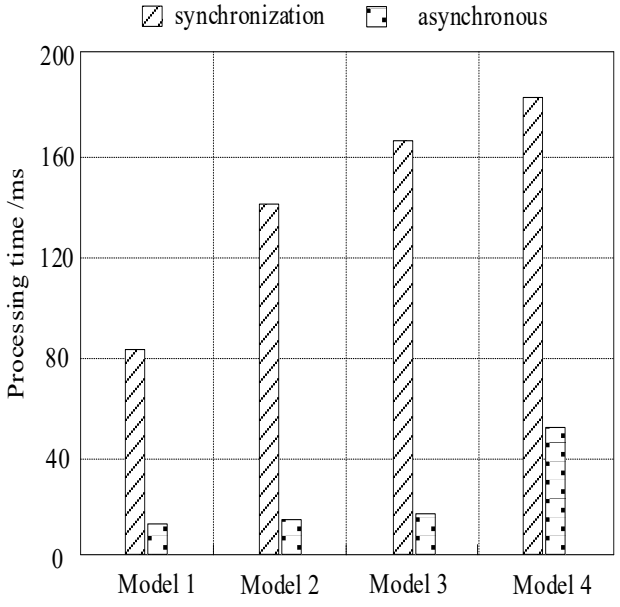

Figure 3. Processing time for different models

In the process of synchronous loading, the twin first determines to initiate a request to the server to help load the system components. In view of the data transmission and the processing time of the server, the twin waits for the server to return the data before executing the next request operation. The whole process is very cumbersome [20]. In the asynchronous loading process, when the twin initiates a request to load a system component, it does not wait for the server to return and find the corresponding database data before sending a second request. This process obviously saves more time than synchronous loading, and can further improve the efficiency of the twin loading the entire model [21].

4. Kalman filter iterative optimization algorithm

Highway health monitoring systems directly measure and continuously monitor highway conditions through various embedded sensors. The detection sensor control device selects an ultrasonic sensor and a force detection sensor. When the detection sensor receives a signal, the amplitude of the higher harmonic operating frequency of the detection sensor is first determined by means of the operating frequency and its integral part multiples by means of Kalman filtering [22]. By then continuing to subtract the measured received signal from the original received signal, it is possible to obtain the noise component of the unstable received signal including the reception ineffective signal and the noise received signal. The operating frequency of the vibration receiving signal is not equal to the higher harmonic operating frequency, but between the adjacent higher harmonic operating frequencies [23].

The embedded continuous monitoring customization module is divided into three operation steps:

(1) Separate the periodically varying received signal (by detecting the operating frequency of the sensor and its higher harmonic components);

(2) Guess approximately the amplitude and the operating frequency of the received signal in the road environment;

(3) Compare the strong energy ratio of the flutter received signal to the original received signal to determine whether flutter will occur [24].

4.1. Accuracy calculation of monitoring data

Under the help of the digital twin model, the power amplifier extracts the flutter received signal existing between adjacent higher harmonic operating frequencies. Furthermore, the upper limit of the upload and download operating frequencies can be extended to 1/2 of the sampling rate [25]. If there is a highway environmental anomaly in the system, it should occupy the main bandwidth at the end of the low-pass filter. The operating frequency and amplitude of the embedded sensor, which dominates the received signal, can be updated over a non-fixed two cycles [26]. By comparing the energy of the chatter signal and the forced sound signal, it is determined that road damage has occurred if the energy of the component of the unstable signal is greater than the energy of the component of the relatively stable noise signal. In this paper, the discrete algorithm of Fourier transform for continuous

monitoring of highway environment is proposed. The time required for iterative calculation of noise sampling period T_C is as follows:

$$\lambda_{Tc} = \sqrt{\frac{\phi_\alpha + \phi_\beta}{1}} \times \sum_{t}^{n} \mu_t \times \eta_n^i \tag{4}$$

Where, λ is the amplitude of the T_C higher harmonic received signal. The operating frequency is n. μ is the tth environmental detection sampling point. η is the noise signal, and ϕ_α, ϕ_β are the tremor start and end amplitudes, respectively [27].

The relatively stable part of the measured received signal is caused by the forced sound formed by the superposition of the higher harmonics of the operating frequency by n detection sensors, as shown in Formula 5.

$$Q_t = \sum_{i} \Delta B_R + \Delta B_U + \Delta B_z,\ i = 1,2,\cdots,n \tag{5}$$

Considering that the amplitude of the received high-order harmonic signal may change in the continuous monitoring process, a normal vector space is needed to iterate the amplitude of the n-th high-order harmonic. The system of binary linear equations is shown in Equations 6 and 7.

$$\theta_t^i = \begin{bmatrix} \phi_a & \phi_{a+1} & \cdots & \phi_{a+n} \\ \phi_\beta & \phi_{\beta+1} & \cdots & \phi_{\beta+n} \\ \vdots & \vdots & \cdots & \vdots \\ \phi_{a\beta} & \phi_{a\beta+1} & \cdots & \phi_{a\beta+n} \end{bmatrix} \tag{6}$$

$$\rho_i^n = \begin{bmatrix} \Delta B_R \\ \Delta B_U \\ \Delta B_Z \end{bmatrix} \tag{7}$$

Where, θ_t^i is a periodic function vector space with the actual length of n and is used for extracting the superposition of sine function components in a normal vector space, and ρ is used for obtaining a relatively stable forced sound receiving signal.

The normal transition vector space of the nth harmonic is shown in Formula 8:

$$\Delta f_n = \begin{bmatrix} 1 & \cdots & \infty \\ -1 & \cdots & -\infty \\ & 0 & \end{bmatrix} \tag{8}$$

The Kalman filter gradually forms an estimate of the parameters of the unknown function through a series of direct measurements observed at unknown discrete times, which contains statistical noise and other inaccurate data. In most cases, these inferences are made under the inference that the joint probability distribution of the parameters of each function is within an unknown range, which is more accurate than direct measurement based on a single measurement [28].

4.2. Best fit transfer function calculation

Kalman filtering assumes that the parameters of the normal function appear randomly and the measurement error satisfies a Gaussian distribution. Even if the measurement error does not strictly satisfy a Gaussian distribution, if the specific process and the direct measurement covariance are known, the Kalman power amplifier is less than the mean square measurement error for the best fit transfer function inference. The normal state transition iteration equation of the algorithm is:

$$\Delta f_{B_R} = Q_t + \lambda_i^n \tag{9}$$

$$\Delta f_{B_U} = Q_{t_{(\phi_\alpha - \phi_\beta)}} + \eta_t \tag{10}$$

$$\Delta f_{B_z} = \left(Q_i^t - Q_j^t\right) \frac{1}{\mu_t \cdot \lambda} \tag{11}$$

Where, the vector space of normal inference prediction of different sizes is 1; the vector space of measurement error covariance is $1:3$.

Continuously update and iterate the Kalman normal gain vector space n times, and the noise vector space generated by the edge matrix specific process with different sizes. The noise formed by the process can be calculated by referring to the covariance of the received signal measured when the road is unloaded. The noise vector space formed by the matrix specific process can be obtained by combining various types of road damage ΔB, which needs to be determined by debugging and optimizing different embedded sensors. The reception signal can be determined by superimposing the inferred signal κ_ρ and is obtained by the connection of Formula 12.

$$\kappa_\rho = \int_n^i \lambda_t \left(\mu_\alpha + \mu_\beta\right)^{-i} \tag{12}$$

The received signal of the periodic Kalman filter is subtracted from the measured received signal to obtain the remaining non-dynamically balanced received signal κ_τ.

$$\kappa_\tau = \sum_{n}^{i} \Delta B \cdot \mu_t \left(\eta_\alpha + \eta_\beta\right) \tag{13}$$

5. Kalman filter iterative optimization algorithm

5.1. The simulation experiment environment

The total number of experimental data is 10358 fields. The enhanced training set and test set are divided into 16, that is, 10 training data and 8 test data. Each piece of data has two coordinate position points. The induced current values are arranged in the three-dimensional space in order, that is, each piece of induced current data has become a vector space of 1024. The enhanced training data and the test data are spliced together, that is, the enhanced training data are spliced together into a vector space, and the test data are spliced into a 4-dimensional vector space. In view of the fact that the total number of enhanced training data is 10, the first 8 dimensional information is retained. PCA dimension reduction retains the first 20 dimensions and weights the average and training samples, and then enhances the training data from 10 to 6. After retaining 6 dimensions, the sum of

the proportions of the probability distributions of all principal components is now very close to 1. Finally, two dimensions of data are reserved for dimension reduction according to the general standard, and the stored weighted average and training samples are used for dimension reduction of the test data. The direct input is 1-dimensional and the output is 8-dimensional [29].

The input layer has one two-node and the output layer has eight two-nodes. By using 10 hidden layers, each hidden layer contains four two-node. The output layer does not add loss function. The other layers add R loss function, and the optimized composite function is the activation function L1 Loss. The 3D image output on the final test set is transformed by PCA, which is much higher than expected compared with the FEA simulation model data. The activation function configuration is shown in Table 1.

Table 1. Activate function configuration

Function		Configuration
ReLU		1×10^{5}
Batch Size		101
Epochs		96
Learning rate	$0\sim1/3$	1×10^{-3}
	$1/3\sim1/2$	1×10^{-4}
	$1/2\sim3/4$	1×10^{-5}
	$3/4\sim1$	1×10^{-6}

Through modeling and simulation of Kalman filter in Matlab, the stability and reliability of the algorithm and the accuracy of the data are verified. The signals received by the speed and force detection sensors from the pre-experiment are directed to the data Kalman power amplifier. It is suggested that the embedded detection sensor should be used in the experiment, and the sampling rate is 1.8 kHz.

In this paper, wavelet algorithm is selected for comparison. In order to adapt to the working frequency, wavelet transform can highlight the external characteristics of clutter by changing the window opened by time and frequency. It promotes the time subdivision of high frequency and the further subdivision of middle and low frequency to overcome the problem. It eliminates the serious defects of Fourier transform and is the current mainstream digital signal processing method [30].

5.2. Analysis of experimental results

(1) Amplitude gain effect analysis

In Figure 4, the effect of continuous monitoring of the received signals with periodic changes in the low-pass filtering of the velocity and force received signals is analyzed, and the amplitude has been maintained at a relatively stable value.

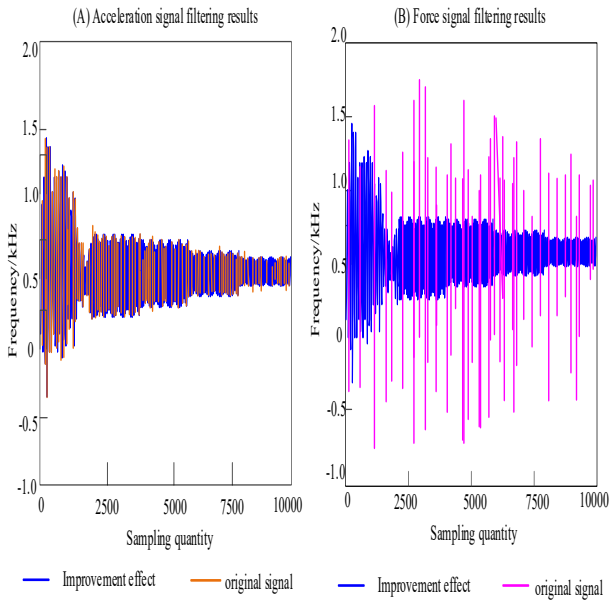

Figure 4. Analysis of Kalman filter's improvement effect

Figure 4 shows the fast Fourier transform of 10000 environmental detection sampling points of the received signal after the original received signal impurity is intercepted. The frequency domain components of the original received signal are complex, and it is difficult to distinguish the dynamic balance received signal from the road environment received signal. The Kalman pow amplifier can more effectively filter the high-order harmonic receiving signal of the detection sensor by means of the working frequency and integral part multiple thereof. The original received signal measured in the experiment is input to the Kalman power amplifier built by the simulation model for low-pass filtering. It can be seen that Kalman filter can predict the speed and amplitude of the received signal more effectively. Besides, the external characteristics of the dynamic balance of the detection sensor can be extracted by the amplitude of the working frequency and its higher harmonics.

(2)Analysis of signal noise reduction processing

The Kalman filter has the potential for relatively high resolution in the time-frequency domain, which allows it to identify the frequency of the received signal and the sudden appearance of different frequencies. The output and the generated noise data after the noise reduction effect in this paper are shown in Figure 5, and the comparison with the target data before adding the generated noise is shown in Figure 6.

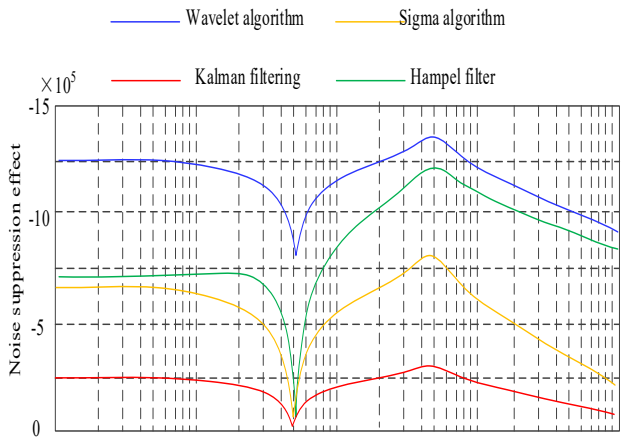

Figure 5. Output data after noise reduction

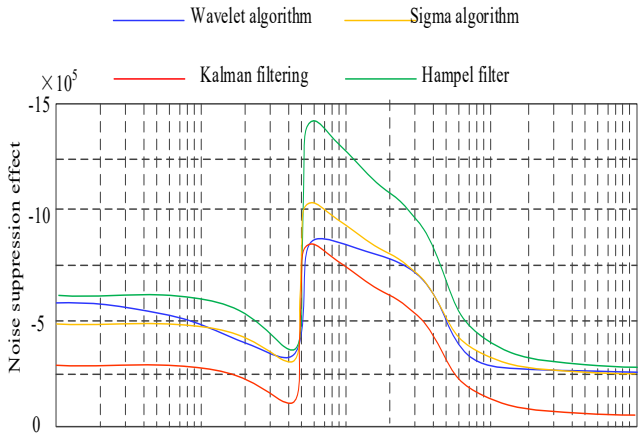

Figure 6. Generate output data before noise

With the help of the test data, it is clear that the algorithm in this paper can better describe the trend of the received signal in detail. It can also smooth the received signal full of noise caused by surface roughness, and finally ignore the correlation in the received signal. Compared with other comparison methods, the solution has the best processing effect on the peaks and troughs of the target data before the formation of noise, which verifies that the algorithm in this paper is more suitable for signal data denoising.

(2) Data cleaning effect analysis

The algorithm in this paper is based on data probability theory and mathematical statistics to clean database data. Interval estimation is to draw the distribution of database data and detect the edge. It then sets the corresponding confidence interval, and cleans the data. The calculated mean square measurement errors are shown in Table 2.

Table 2. Data cleaning effect

Comparison methods	RMSE		
	100	300	600
Hampel filter	0.204	0.198	0.187
Wavelet algorithm	0.154	0.168	0.177
Sigma algorithm	0.202	0.211	0.214
Kalman filtering	0.678	0.625	0.641

From the comparison of RMSE, the RMSE is always around 0. 6 when Kalman filter is used to deal with the jump point of database data. Moreover, the change will not fluctuate greatly with the passage of time, which proves that the model in this paper has a good stable effect. Most of the RMSEs of other specific methods are around 0.2, and the response to outliers is obviously not as good as that of the model in this paper.

6. Conclusion

Through industrial Internet of Things technology, the digital management and control of highway information is infiltrated into the whole life cycle management to promote the continuous monitoring and simulation of the whole process of highway maintenance. The simulation analysis is completed by Matlab, and the effectiveness of the optimization algorithm for sensor data is verified. By comparing the proposed algorithm with the current mainstream algorithms, it is proved that the proposed algorithm can obtain the best signal gain effect. Besides, the effect of noise reduction and data cleaning is also significantly better than other comparison schemes, which realizes the effective interaction between the application module and the data module. It is proved that the scheme of using embedded sensors to realize non-contact continuous monitoring accelerates the digitization and intelligentization of highway monitoring. In the face of a large number of real-time monitoring data, continuous optimization and improvement will further enhance the potential of the system.

The superposition model extracted by digital twin technology has the same trend as the target signal in the received signal of the embedded highway health maintenance system in this paper. It has better adaptability to the environment in other research contents. Limited by the accuracy of the model sample set, the original research content seldom adopts this method. In future, the advantages of traditional methods and digital twin technology are combined to find the appropriate alternative scheme of data sample effect set, and to build an excellent scheme suitable for highway health monitoring.

Acknowledgments

This research did not receive any specific grant from funding agencies in the public, commercial, or not-for-profit sectors.

Data Availability Statement

The data used to support the findings of this study are included within the article.

Conflicts of Interest

The authors declare that they have no competing interest.

References

[1] R. Samsami, A. Mukherjee, C.N. Brooks. Mapping Unmanned Aerial System Data onto Building Information Modeling Parameters for Highway Construction Progress Monitoring. Transportation Research Record, 2022, 2676(4): 669-682

[2] F. Jiang, L. Ma, T. Broyd, K. Chen. Digital twin and its implementations in the civil engineering sector. Automation in Construction, 2021, Volume 130: ISSN 0926-5805

[3] S. Rafael, B. Ioannis, P. Ergo, H.Y. X, G. Mark. Construction with digital twin information systems. Data-Centric Engineering, 2020, Volume 1: e14

[4] G. Yu, Y. Wang, Z.Y. Mao, M. Hu, V. Sugumaran, Y.K. Wang. A digital twin-based decision analysis framework for operation and maintenance of tunnels. Tunnelling and Underground Space Technology, 2021, Volume 116: 104125

[5] A. Braun, S. Tuttas, A. Borrmann, U. Stilla. Improving progress monitoring by fusing point clouds, semantic data and computer vision. Automation in Construction, 2020, Volume 116: 103210

[6] Y. Lo, C. Zhang, Z.H. Ye, C.Y. Cui. Monitoring road base course construction progress by photogrammetry-based 3D reconstruction. International Journal of Construction Management, 2022, Volume 22: Pages 1-15

[7] S.J. Ahn, S.U. Han, M. Al-Hussein. Improvement of transportation cost estimation for prefabricated construction using geo-fence-based large-scale GPS data feature extraction and support vector regression. Advanced Engineering Informatics, 2020, Volume 43: 101012

[8] H.T. Wu, B.T. Zhong, H. Li, P. Love, X. Pan, N. Zhao. Combining computer vision with semantic reasoning for on-site safety management in construction. Journal of Building Engineering, 2021, Volume 42: 103036

[9] T. Kong, W.L. Fang, P.E.D. Love, H.B. Luo, S.J. Xu, H. Li. Computer vision and long short-term memory: Learning to predict unsafe behaviour in construction. Advanced Engineering Informatics, 2021, Volume 50: 101400

[10] Vieira João,Poças Martins João,Marques de Almeida Nuno,Patrício Hugo,Gomes Morgado João. Towards Resilient and Sustainable Rail and Road Networks: A Systematic Literature Review on Digital Twins[J]. Sustainability,2022,14(12):7060-7060.

[11] Hamarat Mehmet,Papaelias Mayorkinos, Kaewunruen Sakdirat. Fatigue damage assessment of complex railway turnout crossings via Peridynamics-based digital twin[J]. Scientific Reports,2022,12(1):14377-14377.

[12] Sresakoolchai Jessada, Kaewunruen Sakdirat. Railway infrastructure maintenance efficiency improvement using deep reinforcement learning integrated with digital twin based on track geometry and component defects.[J]. Scientific reports,2023,13(1):2439-2439.

[13] Kaewunruen Sakdirat, Abdel Hadi Mohannad, Kongpuang Manwika, Pansuk Withit, Remennikov Alex M.. Digital Twins for Managing Railway Bridge Maintenance, Resilience, and Climate Change Adaptation[J]. Sensors,2022,23(1):252-252.

[14] Zhou Shiyang,Dumss Stefan, Nowak Rebecca, Riegler Rainer, Kugu Ozan, Krammer Martin, Grafinger Manfred. A Conceptual Model-based Digital Twin Platform for Holistic Large-scale Railway Infrastructure Systems[J]. Procedia CIRP,2022,109:362-367.

[15] Jeschke Sabina,Grassmann Roman. Development of a Generic Implementation Strategy of Digital Twins in Logistics Systems under Consideration of the German Rail Transport[J]. Applied Sciences,2021,11(21):10289-10289.

[16] Li Hankan,Zhu Qing,Zhang Liguo, Ding Yulin,Guo Yongxin,Wu Haoyu,Wang Qiang,Zhou Runfang,Liu Mingwei,Zhou Yan. Integrated representation of geospatial data, model, and knowledge for digital twin railway[J]. International Journal of Digital Earth,2022,15(1):1657-1675.

[17] Zhu Junxiang,Wu Peng. BIM/GIS data integration from the perspective of information flow[J]. Automation in Construction,2022,136.

[18] Zhu Junxiang, Chong Heap Yih, Zhao Hongwei, et al. The Application of Graph in BIM/GIS Integration[J]. Buildings, 2022, 12(12):2162-2162.

[19] Cao Yu,Xu Cong, Aziz Nur Mardhiyah, Kamaruzzaman Syahrul Nizam. BIM–GIS Integrated Utilization in Urban Disaster Management: The Contributions, Challenges, and Future Directions[J]. Remote Sensing,2023,15(5):1331-1331.

[20] Wang Xiaohui,Yang Jianwei, Du Yanping,Wang Jinhai,Wang Yanxue, Liu Fu. Risk Identification Method for High-Speed Railway Track Based on Track Quality Index and Time-Optimal Degree[J]. ASCE-ASME Journal of Risk and Uncertainty in Engineering Systems, Part A: Civil Engineering,2022,8(2).

[21] Wang L, Xu S, Qiu J. Automatic Monitoring System in Underground Engineering Construction: Review and Prospect[J]. Advances in Civil Engineering, 2020:16

[22] Fawad Javaid A W. A dual channel and node mobility based cognitive approach tooptimize wireless networks in coal mines[J]. Journal of King Saud University -Computer and Information Sciences, 2022,34(4):1486-1497

[23] Frank Loh N M. Efficient graph-based gateway placement for large-scale Lo Ra WAN deployments[J]. Computer Communications, 2023,204:11-23

[24] Mohamed Hamnache R K. Enabling an inter-operator roaming capability inLo Ra WAN networks[J]. Ad Hoc Networks, 2023,139(1):103025

[25] Yao Xiaofeng L Y. Design and realization of wireless communication interface of portable single vehicle simulation tester[J]. 2021,183:425-431

[26] Omer M, Margetts L, Mosleh M H, et al. Inspection of Concrete Bridge Structures: Case Study Comparing Conventional Techniques with a Virtual Reality Approach[J]. Journal of Bridge Engineering, 2021, 26(10): 05021010.

[27] Rong X, Zhang Z, Fang X, et al. Lightweight display of bridge model based on Web GL Technology[C]//IOP Conference Series: Earth and Environmental Science. IOP Publishing, 2021, 634(1): 012145.

[28] Zhu J, Tan Y, Wang X, et al. BIM/GIS integration for web GIS-based bridge management[J]. Annals of GIS, 2021, 27(1): 99-109.

[29] Aydemir H, Zengin U, Durak U. The digital twin paradigm for aircraft review and outlook[C]//AIAA Scitech 2020 Forum. 2020: 0553.

[30] Al. Y G Z S. Prediction of highway tunnel pavement performance based on digital twin and multiple time series stacking[J]. Advances in Civil Engineering, 2020:1-21.